Wireless Power Transfer for Space Applications

Gabriel Vazquez Ramos[1] and Jiann-Shiun Yuan[2]

[1]National Aeronautics and Space Administration
Launch Services Program (Mail Code: VA-H3)
John F. Kennedy Space Center, FL 32899
[2]Department of Electrical Engineering and Computer Science
University of Central Florida, Orlando, FL 32816

Abstract: This paper introduces an implementation for magnetic resonance wireless power transfer for space applications. The analysis includes an equivalent impedance study, loop material characterization, source/load resonance coupling technique, and system response behavior due to loads variability. System characterization is accomplished by executing circuit design from analytical equations and simulations using Matlab and SPICE. The theory was validated by a combination of different experiments that includes loop material consideration, resonance coupling circuits considerations, electric loads considerations and a small scale proof-of-concept prototype. Experiment results shows successful wireless power transfer for all the cases studied. The prototype provided about 4.5 W of power to the load at a separation of ~5 cm from the source using a power amplifier rated for 7 W.

Keywords: magnetic coupling, magnetic resonance, power transfer, space systems, wireless power

1. Introduction

For space systems, power connectors constitute a vital and complicated component required for the success of every space mission. Some of these missions require crucial connector mate and de-mate operations in an environment full of contaminants and/or performed by an automatic (unmanned) systems. These operations can constitute a risk of lost of mission due to connector deterioration after been exposed to environmental contaminates (i.e., lunar regolith, also call moon dust) or by bended pins due to misaligning during a connector mate operation [1]. To mitigate these concerns, the design of a wireless power transfer (WPT) system for space applications is desirable.

In classical physics, mechanical resonance has been widely demonstrated in various applications and examples (i.e., identical tuning forks resonanace). In 2007, a research team from MIT demonstrated a similar principle on electric circuits called magnetic resonance (also known as magnetic coupling) [2].

In this paper, a WPT system is proposed to transfer electric power without the need of having physical electrical connection. The intent of this design is to have a modular approach that can be used as a wireless power connector for a wide range of space exploration applications such as automatic docking systems for space systems rendezvous, wireless sensors for launch vehicles, and robotic mission charging stations on other planets, moons and asteroids. The main scope of this work is to provide a simple design approach for the implementation of a WPT and its feasibility for space applications with a circuit analysis emphasis on the resonance coupling circuit and load interaction. Therefore, a lightweight "small" resonance coupling system (using hollow inductors) will be implemented to avoid adding excessive weight to the launch vehicle

applications and a low-to-medium range (3-7 cm) of nominal power transfer distance will be evaluated to avoid interference with adjacent launch vehicle and spacecraft avionics systems.

2. Theory

Based on technical literature review and component level testing, a simple design approach is delineated for the analysis and fabrication of the wireless power transfer devices. Block diagrams are shown in Fig. 1, demonstrating the main elements required for the WPT system implementation [3].

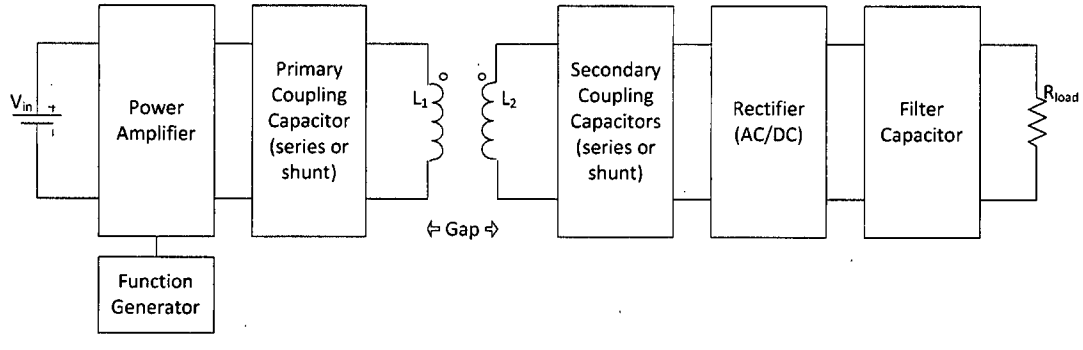

Fig. 1. WPT systems block diagram

Overall System Operation

An electric source circuit generates a square wave or sinusoidal signal (represented by a power amplifier in Fig. 1) inducing magnetic pulsation signals at the primary loop (L_1) of the source resonant circuit. The secondary loop will receive the magnetic pulses of L_1 due to the fact that is part of the secondary resonant circuit (C_2 and L_2). The secondary resonanting circuit is tuned to the same frequency as the source circuit. This magnetic energy induces a sinusoidal electric signal in the secondary [2]. The alternate current (AC) signal is then rectified by a diode

H-bridge and a filter capacitor to provide a direct current (DC) signal to the load. This process will transfer energy wirelessly from the primary circuit (source) to the secondary circuit (load) [2].

The overall system analysis and design was performed by a systematic series of simulations using the combination of Matlab, MathCAD, ADS, and LTSPICE software packages. This integrated system circuit simulation combines different technical topics evaluated for the design. These topics were divided into three main design simulations categories: WPT resonance coupling circuit design/simulation, WPT system circuit simulation and WPT equivalent impedance characterization. Each of these simulations provides an important contribution for the overall understanding of the system's electrical behavior.

Resonance Coupling Circuits Design/Simulation:

The WPT magnetic coupling elements are defined as the primary and secondary loops with their respective (primary and secondary) coupling capacitor (see Fig. 1) for resonant circuit filtering. To determine the magnetic element parameters, a MathCAD based code was devloped using simple electromagnetic and circuit equations. This tool helps us understand how to design the inductor loops and their corresponding coupling capacitor for the desired operating frequency. There are four capacitor coupling configurations combinations that will be described and analyze later; however, the various capacitor coupling configuration does not affect the following coupling definitions.

The self inductance of the inductor loop with no magnetic core is defined as [4]:

$$L = N^2 R \mu_0 \left[\ln\left(\frac{8R}{r}\right) - 1.75 \right] \tag{1}$$

where N is the number of turns in the loop, R is the radius of the loop, μ_0 is the permeability of vacuum, and r is the loop conductor resistance. Eq. (1) provides a good approximation of the loop inductance. However, an exact value is not expected due to manufacture variability. For a precise inductance characterization, it is recommended to measure the inductance with an LCR meter with the established operational frequency.

In order to adequately transfer power wirelessly, the primary and the secondary magnetic loops need to be tuned to the same resonant frequency. One of the tuning techniques is accomplished by connecting a capacitance in series to the primary circuit and in parallel to the secondary circuit (also known as series-parallel coupling) [3]. The other three coupling techniques are illustrated in Fig. 1. Eq. (2) is utilized to determine the capacitor value required to generate the resonant circuit with the inductor [5]:

$$C = \frac{1}{\omega_0^2 L} \tag{2}$$

where C is the coupling capacitance required, ω_0 is the frequency of oscillation [rad/sec], and L is the inductance of the coil. An approach implemented to overcome inaccuracy in the inductance calculation or non-exact capacitor value, would be to design symmetrical loops (primary and secondary) and run a magnetic element frequency sweep to determine the best coupling frequency through experimentation.

An additional calculation to be considered is the mutual inductance between the two loops. This value will be calculated for the required separation distance of the gap between the primary and the secondary, and will be use on the SPICE circuit analysis to determine the overall circuit

response. Before calculating the mutual inductance, it is required to determine the magnetic coupling coefficient k as follows [6]:

$$k = \frac{1}{\left[1 + 2^{2/3} \frac{D^2}{R_1 R_2}\right]^{3/2}} \tag{3}$$

where D is the physical distance between the first and second inductors (gap), R_1 is the radius of the loop 1, and R_2 is the radius of the loop 2. As mentioned in [6] this equation is intended for "close-to-medium" proximity coupling.

By using the magnetic coupling coefficient, a characterization of the mutual inductance L_M is given by [7]:

$$L_M = k\sqrt{L_1 L_2} \tag{4}$$

where L_1 is the inductance of the loop 1 and L_2 is the inductance of the loop 2.

WPT System Circuit Simulation

To characterize the overall circuit performance, it was required to find a circuit model that can help predict the performance of the overall system other than the standard k factor model between the two loops. The additional model used to emulate the behavior of the two hollow inductor loops (under magnetic resonance) is the non-ideal transformer equivalent circuit [8] with SPICE simulation as well as simulation based on the coupling coefficient using Agilent's ADS.

By implementing the coupling coefficient characterization approach and validated by the non-ideal transformer equivalent circuit, the overall circuit was simulated. Fig. 2 illustrates the four possible coupling configurations to be studied. A square wave voltage source is used as the input voltage (emulating the PA input to the WPT system as shown in Fig. 1).

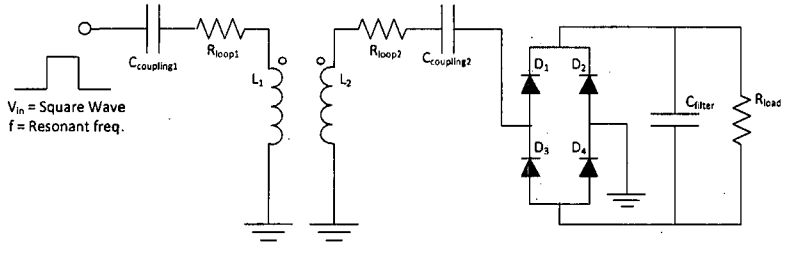

(a)

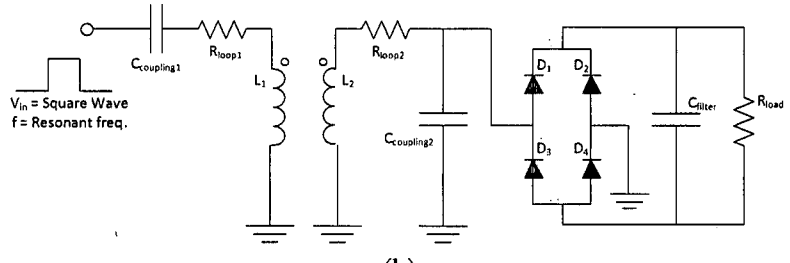

(b)

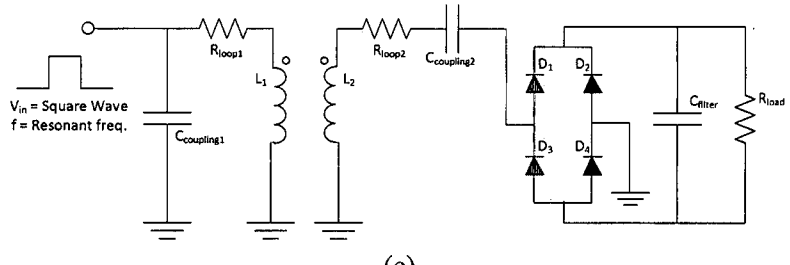

(c)

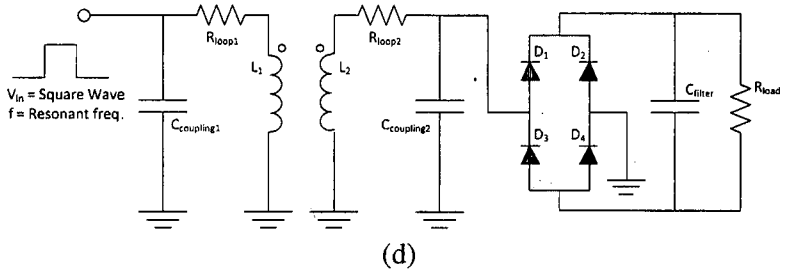

(d)

Fig. 2: Simulated wireless power transfer models: (a) series-series coupling, (b) series-shunt coupling, (c) shunt-series coupling, and (d) shunt-shunt coupling.

Circuit details are taken for the proof-of-concept-prototype and will be discussed in Section 3. The circuit's primary side coupling is considered to be very dependent on the application. However; series compensation is considered to be the best configuration for power supply voltage [3]. Shunt configuration in the primary represents a reduction on supplied current, a condition desirable for large power WPT [3]. The circuit's secondary side coupling is simpler to interpret: the series coupling corresponds to a voltage source characteristic in the secondary while the parallel coupling corresponds to current source characteristics [3].

WPT Equivalent Impedance Characterization

An additional consideration studied to enhance the understanding of the overall system electrical behavior was to determine the equivalent impedance of the system connected to the source. A circuit simplification code was developed in Matlab to determine the equivalent impedance of the magnetic element and the load (given the design and calculated circuit values). Fig. 3 illustrates the definition of the equivalent impedances for the series-shunt and series-series coupling circuits without the rectifier in the output. For the purpose of evaluating equivalence impedance, the effect of the output rectifier was not taken into account. The equivalent impedance analysis was only performed to the two configurations of interest for our WPT application. The leakage inductances ($L_{leakage1}$ and $L_{leakage2}$) can be determined by the respective inductance value (L_1 or L_2) minus the mutual inductance (L_m). The loop resistances R_{loop1} and R_{loop2} represent their respective inductor series resistances.

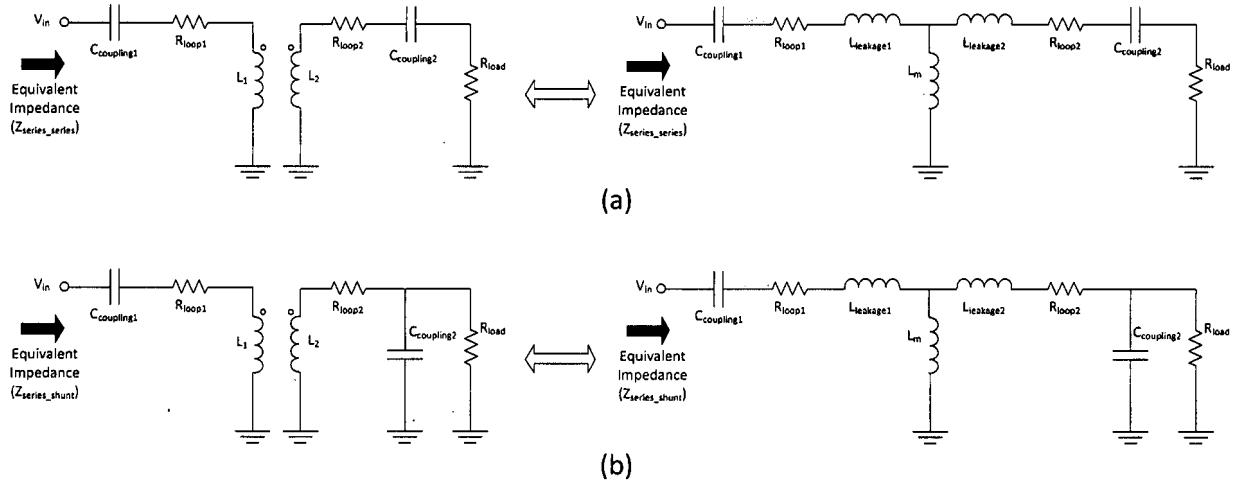

Fig. 3 Circuits used to determine equivalent impedance: (a) series-series coupling configuration and (b) series-shunt coupling configuration

The equivalent impedances of the circuits shown in Fig 3 were determined. Eq. (5) is the calculated equivalent impedance representation of the WPT system series-series coupling configuration and Eq. (6) is the calculated equivalent impedance representation of the WPT system series-shunt coupling configuration.

$$Z_{series-series} = R_{loop1} + sL_{leakage1} + \frac{1}{sC_{coupling1}} + \frac{1}{\frac{1}{R_{loop2} + R_{load} + sL_{leakage2} + \frac{1}{sC_{coupling2}}} + \frac{1}{sL_m}} \tag{5}$$

$$Z_{series-shunt} = R_{loop1} + sL_{leakage1} + \frac{1}{sC_{coupling1}} + \frac{1}{\frac{1}{R_{loop2} + sL_{leakage2} + \frac{1}{sC_{coupling2} + (1/R_{load})}} + \frac{1}{sL_m}} \tag{6}$$

3. Results and Discussion

A proof-of-concept prototype was assembled to demonstrate the theory proposed. The parameters used in the proof-of-concept prototype are listed in Table 1. Using the equations provided in Section 2, coupling capacitors, self inductance of the loops and mutual inductance parameters were calculated and listed in Table 2.

Table 1: Proof-of-concept prototype characteristics

Parameter	Symbol	Value	Units
Number of turns	N_1 & N_2	8	turns
Radius of the Loops	R_1 & R_2	0.24	m
Loop conductor radius	r_1 & r_2	~ 0.001	m
Loop conductor resistance (for 20 kHz)	a	~ 0.4*	Ohm
Frequency of operation	f_0	23	kHz
	ω_0	144.5	kRad/s
Vacuum Permeability	μ_0	$4\times\pi\times10^{-7}$	H/m
Separation distance	D	0.03	m
Load	R_{load}	2.5	Ohms

*Average value of the inductor loop materials under study

Table 2: Calculated prototype circuit parameters

Parameter	Symbol	Value	Units
Self Inductance	L_1 & L_2	49.38	μH
Mutual Inductance	L_m	42.85	μH
Coupling Capacitor	C_1 & C_2	1*	μH
Leakage Inductances	L_{lk1} & L_{lk2}	6.533	μH

* Mylar capacitors of 1 μF (10% accuracy) were used.

Applying the equations provided in Section 1, SPICE simulations were executed for the coupling configurations listed in Fig. 2. This provides a good snapshot on which coupling configuration could offer the greatest power transfer for our application. It can be seen in Fig. 4 that the best coupling configurations are series-series and series-shunt coupling.

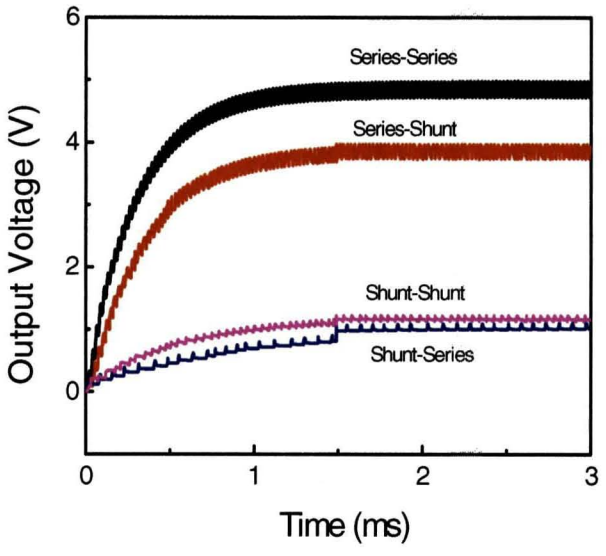

Fig. 4 WPT system simulation for various coupling configurations

A test setup was developed to execute various WPT test cases and circuit variations (see Fig. 5). This test setup helps vary the distances of the loops to take output voltage and power measurements.

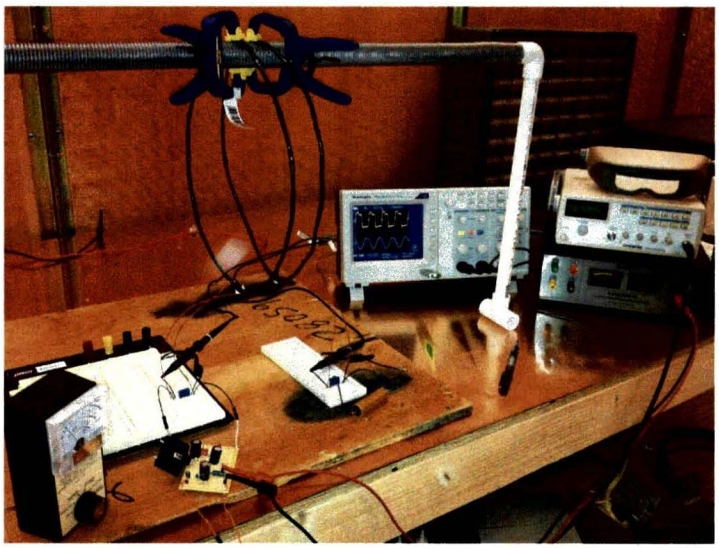

Fig. 5 WPT system test setup

Equivalent Impedance Characterization Results

Using Eqs. (5) and (6) results and the prototype values provided in Tables 1 and 2, the equivalent impedances values for both cases (series-series and series-shunt) fluctuates for distances less than ~5 cm. However, for distances greater than 5 cm the equivalent impedance consistently decreases value. A possible explanation for this behavior is that at about 5 cm the system reaches the critical coupling case. Therefore, for separation distances of less than 5 cm the system could be considered to be in an over-coupling condition and for separation distances greater than 5 cm the system could be considered to be in an under-coupling configuration. These concepts are thoroughly explained in references [9] and [10].

Experiment #1: ***Inductor Loop Characterization***

Inductor loops used for the resonance circuits could be considered to be one of the most important and complex parts to develop the proposed WPT systems. Depending on the specific characteristics of these loops, and their construction, wireless power transfer can be maximized

and optimized. To evaluate the design and construction of the loop inductors and their contribution to the overall coupling, different conductor materials where evaluated. Solid conductor, speaker wire (braided naked wire inside a single insulator) and litz wire (individual insulated wires than are later braided) where selected to design same-size and same-number-of-turns inductors to establish a WPT comparison. For each conductor material a pair of loops was developed in order to evaluate the system behavior with identical conductor material. All the conductors used for this experiment are around AWG 24 or equivalent to establish adequate comparison between the materials.

The inductance value of the developed inductor loops for various frequencies of operation is illustrated in Fig. 6. These values were captured using an Agilent 4980A LCR Meter. It can be noticed that at low frequencies the calculated values using Eq. (1) are reasonably similar to the inductor loop values measured. The speaker and litz wires had considerably closer inductance values to the calculated ones. Fig. 7 illustrates the quality factor (Q) value of the developed loops for various frequencies of operation. This figure shows how the litz wire has a greater Q for lower frequencies, meaning that it will have less series resistance than the other two conductors. Therefore, the litz wire implementation could be favorable for the proof-of-concept-prototype at the targeted frequency of 20 kHz.

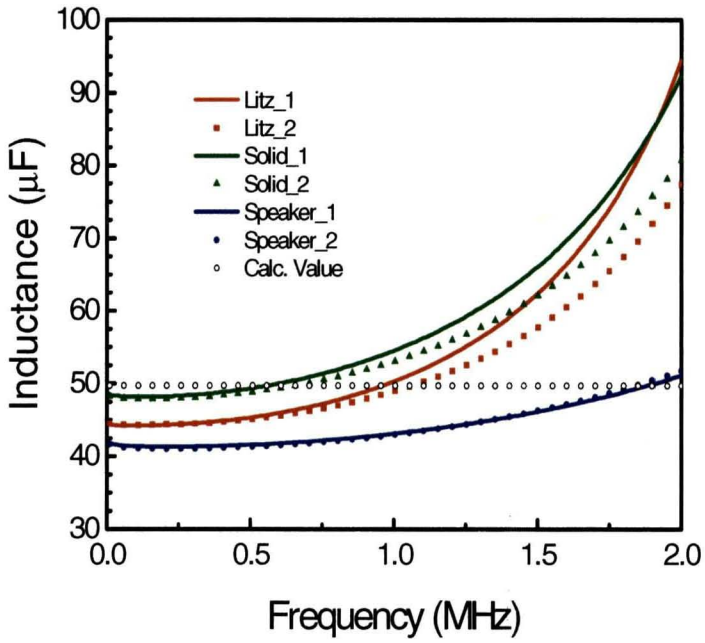

Fig. 6 Loops inductance with respect to the frequency of operation

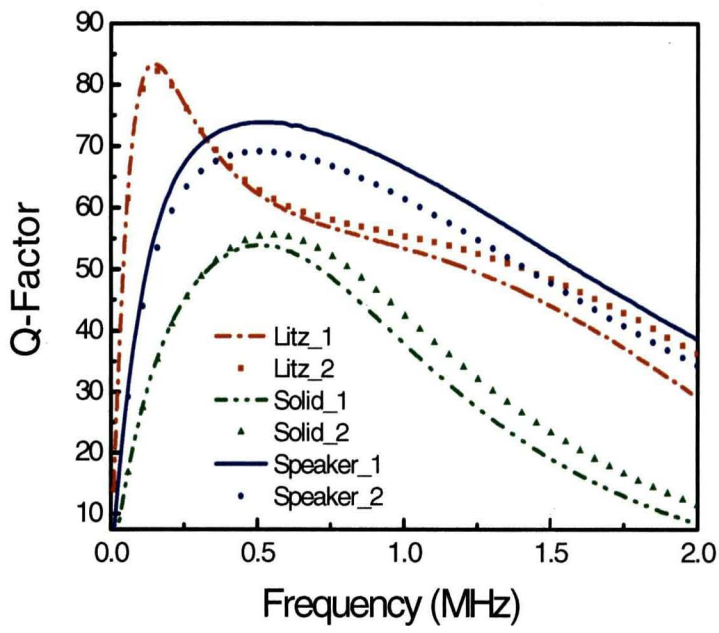

Fig. 7 Loops quality factor with respect to the frequency of operation

One of the parameters required to determine the overall system behavior, according to Section 2, is the loop series resistance. An accurate value of the series resistance can be obtained by using Eq. (7) [9]. Table 3 provides the calculated results of the series resistance for all the inductors at an operational frequency of 20 kHz.

$$R_S = \frac{wL}{Q} = \frac{(2\pi f)L}{Q} \tag{7}$$

Table 3: Calculated inductor loop series resistance at 20 kHz

Inductor Loop	Inductance (uH)	Q factor	R_S (Ω)
Litz wire 1	44.3	27.1	0.205
Litz wire 2	44.4	26.3	0.212
Solid wire 1	48.3	6.1	0.995
Solid wire 2	48.1	6.0	1.007
Speaker wire 1	41.7	12.2	0.430
Speaker wire 2	41.5	11.7	0.446
Average	44.7	14.9	0.377

As Eq. (7) suggests, the lowest series resistance is provided by the material with the highest Q-value. For the three inductor loop materials analyzed, the litz wire was the conductor that provided a greater Q-factor for the same-size and same-number-of-turns comparison.

Experiment #2: *WPT Fix Separation Distance Considerations*

Aiming to reaching the greater understanding of the WPT systems, multiple parameters and test configurations were evaluated with a fixed distance of 3 cm. Some of the varied parameters where: loop material, coupling configuration (Fig. 2) and load resistance (2.5 Ω, 4 Ω and 8 Ω).

These resistance values were selected due to the fact that the power amplifier used for the experimentation was designed to be optimal for 4 Ω loads [11]. This experiment was performed by implementing the circuits described in Fig. 2. The combination of test sets acquired by varying the parameters previously mentioned generates a significant amount of data.

Data reflected that the greatest power transfer was provided by having an output load of 2.5 Ω, coupling configuration of series-shunt and having litz wire as the inductor loop material.

Experiment #3: *WPT Variable Separation Distance Considerations*

The purpose of this experiment is to characterize the system behavior based on separation distance, coupling configuration and load (output resistance). This experiment was divided into two parts: identification of coupling configuration of interest and characterization of the system behavior for the coupling configuration of interest. Each part provides specific characterization of the overall system behavior.

Part 1: Identification of Coupling Configurations of Interest

The first part of this experiment was performed as a pathfinder test to narrow down the coupling configuration of interest to validate the results in the previous sub-section (Fig. 4). This helps reduce the amount of data required for the second part. The characterization is perfumed with the best inductor loop material identified so far based in experiment #1 (litz wire loops) in combination with the load resistance value (4 Ω) consider optimal of the PA selected for experimentation [11]. The litz wire material is considered to be the best material of the three analyzed due to the fact that it shows a higher Q for the desired frequency (~20 kHz). However, detailed characterization of the other loop materials will be performed on part 2 of this experiment. Circuits were assembled according to Fig. 2 and results are illustrated in Fig. 8.

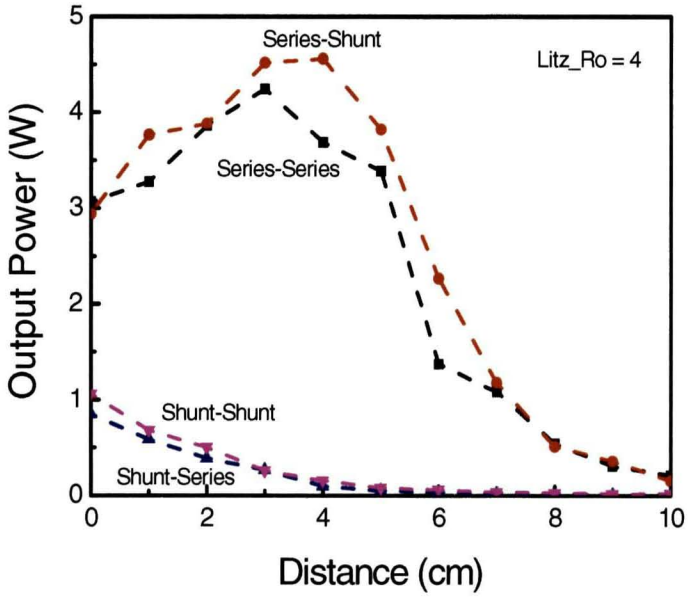

Fig. 8 Coupling configuration pathfinder results using litz inductor loops for a 4 Ω load

It is clear from Fig. 8 that the configurations that provide the greatest output power for this WPT application are: series-series and series-shunt coupling. Therefore, for the second part of this experiment, the system behavior characterization will be based on these two coupling configurations. As previously simulated, the primary series coupling configuration provide greater current to the WPT [3]. This condition is favorable for our low-to-medium power application; however, for high power applications the primary coupling configuration could be implemented in parallel to reduce the input currents.

Part 2: Characterization of the System Behavior

The second part of this experiment is to vary the coupling configurations of interest determine on the first part of this experiment. It was identified that the coupling configuration of interest

are: series-series and series-shunt. Other than the coupling configuration, the inductor loop material and load values will be evaluated as well.

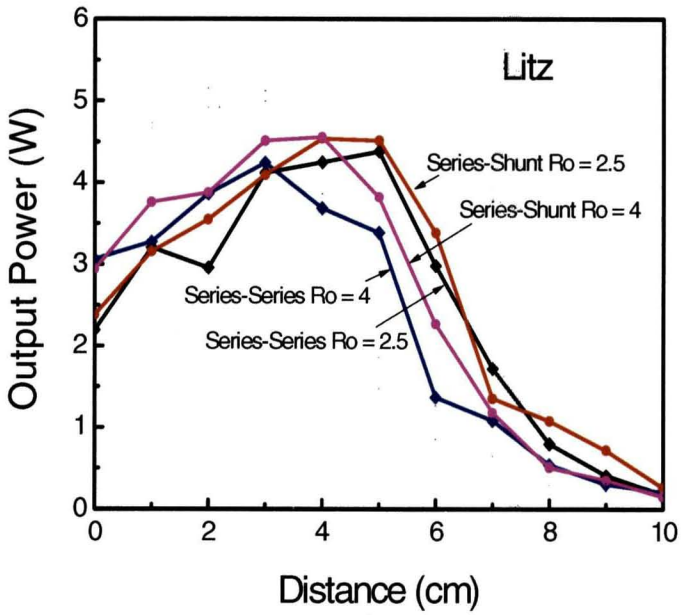

(a)

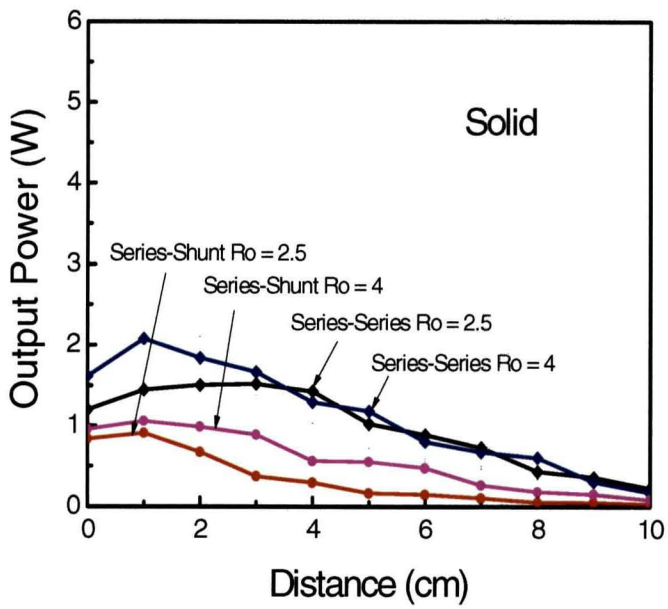

(b)

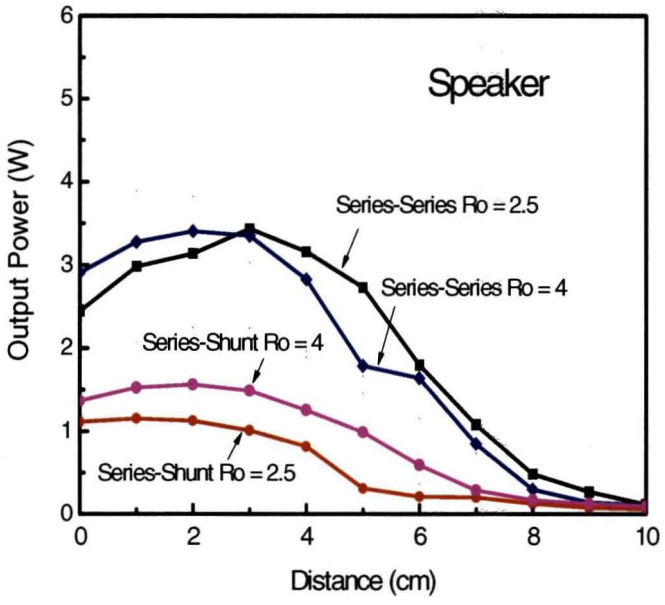

(c)

Fig. 9 WPT system output power for variable separation distance: (a) litz wire loops, (b) solid wire loops and (c) speaker wire loops.

It can be seen in Fig. 9 that the litz wire inductor loop provides the greatest power transfer for all the resistances studied and the coupling configurations of interest. It is also noticed that the worst inductor loop material for this specific WPT application is the solid wire. A common characteristic that the two best materials (litz and speaker wire) share is having braided conductors. This helps prevent skin effect losses within the cable that could generate energy leakages [12]. However, by the litz wire having insulated conductors before been braided as a cable, it is believed that this provides considerable advantages over the speaker wire according to the performance demonstrated in Fig. 9. Therefore, the proof-of-concept prototype will be using litz wire as the inductor loop material.

Proof-of-Concept Prototype

A proof-of-concept prototype was assembled to validate the design approach discussed in Section 2. The prototype envelopes the cases studied for: inductor wire material, coupling configuration and load analysis. It was determined, based on analysis and experimentation, that the best case scenario used for the Proof-of-Concept Prototype was: 2.5Ω load, coupling configuration of series-shunt and litz wire as the inductor loop material.

For the construction/testing of the prototype, multiple test equipments, electronic parts and components were evaluated and selected to emulate the overall WPT system (see Fig. 1). Since the main scope of this project was to emphasize on inductor loop wire material, coupling configuration and load variability, laboratory test equipment was used to cover the other functions required by the WPT system.

It can be noticed that the greatest power transfer occurs at ~5 cm (see Fig. 10). Data shows a prototype output power of 4.5 W using a Power Amplifier rated for 7 W [11].

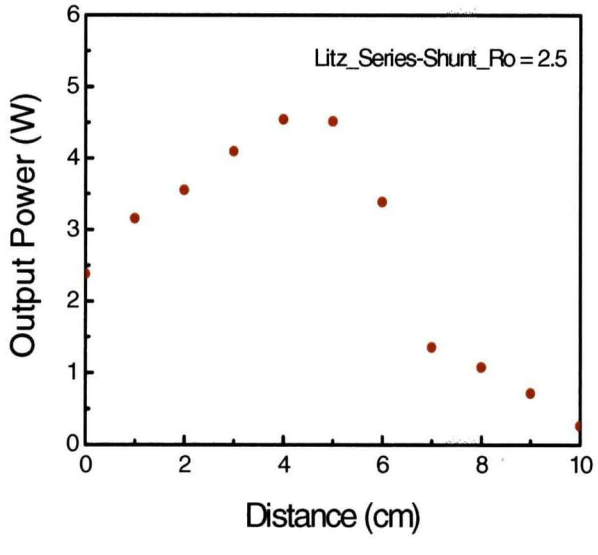

Fig. 10 WPT system prototype power output

The system operating frequency (f_0) was targeted to be 23 kHz. Discrepancies between design frequencies and system tunned frequency can be encountered at the prototype phase. This can be due to the coupling capacitor tolerance, the loop conductor radius measurement and the variability of the manually built inductor loops. An accurate representation of the loop conductor radius and coupling capacitor values are required for an accurate system coupling according to Eqs. (1) to (3).

Additional testing was performed to the prototype by adding non-conductive material between the source element and the load element (i.e. carbon-fiber, wood, plastic, etc). As expected, magnetic coupling was achieved even through non-conductive materials.

4. Conclusion

Based on theoretical analysis and experimental results, magnetic resonance is a feasible and reliable technology that represents an alternative to conventional electric connectors. Simulation and prototype testing enabled us to establish the best configurations for the WPT parameter studied: inductor loop material, capacitor coupling configuration and loads variation.

By evaluating multiple inductors loop materials (litz, solid and speaker wire), it was noticed that the litz wire presented an advantage against the other materials studied. This is due to multiple individual insulated conductors before been braided as a cable, which helps prevent skin effect losses within the cable that could generate energy leakages.

The capacitive coupling configurations that generate the best results for our WPT application were: series-series and series-shunt. This is attributed to the fact that the primary series coupling configuration provide greater current to the WPT system.

Preliminary testing also showed that magnetic resonance can be achieved through non-conductive materials (i.e. wood, plastic, etc). Multiple mobile devices can be powered at the same time using a single source. This was accomplished by tuning the source and all the loads to the same operating frequency. In addition, it was demonstrated by prototype experimentation that magnetic resonance can be achieved within audible frequencies (20 Hz $\leq f_0 \leq$ 20 kHz). This can represent a major industrial advantage due to the fact that there are currently a wide range of options available for audio power amplifiers.

More testing and experimental data will be required for the implementation of a reliable and efficient wireless power system for space applications. In theory, the magnetic resonance principle is believed to operate in the space environment. However, using the principles discussed in this paper and additional analysis, a more advanced design will be evaluated for compliance to NASA and other military systems standards [13-16]. Design compliance to these standards will be highly dependent on the system application (i.e., launch vehicles, spacecraft, rover, wireless battery charger, docking systems, etc.).

REFERENCES

[1] National Aeronautics and Space Administration *Workmanship Problems Pictorial Reference/Wiring and Cabling* NASA Electric Parts and Packaging Program (Online) *URL: http://nepp.nasa.gov/index.cfm/14257*

[2] A. Karalis, J. D. Joannopoulos, and M. Soljacic, "Efficient wireless non-radiative mid-range energy transfer," *Annals of Physics*, vol. 323, pp. 34-48, 2008.

[3] O. H. Stielau and G. A. Covic, "Design of loosely coupled inductive power transfer systems," *Int. Conf. Power System Technology*, 2000, pp. 85-90.

[4] C. Zhu, K. Liu, C. Yu, R. Ma, and H. Cheng, "Simulation and experimental analysis on wireless energy transfer based on magnetic resonances," *Vehicle Power and Propulsion Conference,* 2008, pp. 1-4

[5] C. Zhu, C. Yu, K. Liu, and R. Ma, "Research on the topology of wireless energy transfer device," *Vehicle Power and Propulsion Conference,* 2008, pp. 1-5.

[6] J. O. Mur-Miranda, G. Fanti, F. Yifei, K. Omanakuttan, R. Ongie, A. Setjoadi, and N. Sharpe, "Wireless power transfer using weakly coupled magnetostatic resonators," *IEEE Energy Conversion Congress and Exposition*, 2010, pp. 4179-4186.

[7] H.S. Kim; D. H. Won, B.-J. Jang, "Simple design method of wireless power transfer system using 13.56MHz loop antennas," *IEEE Int. Symp. Industrial Electronics*, 2010, pp.1058-1063.

[8] S. Judek and K. Karwowski, "Supply of electric vehicles via magnetically coupled air coils," *IEEE Power Electronics and Motion Control Conference,* 2008, pp.1497-1504.

[9] Bowick, Christopher, Cheryl Ajluni, and John Blyler. RF Circuit Design, Second Edition. Newnes, © 2008.

[10] Sample, A.P.; Meyer, D.A.; Smith, J.R.; , "Analysis, Experimental Results, and Range Adaptation of Magnetically Coupled Resonators for Wireless Power Transfer," Industrial Electronics, IEEE Transactions on , vol.58, no.2, pp.544-554, Feb. 2011

[11] Velleman Components NV. *7W Mono Amplifier, Kit.* Velleman Components NV. K4001.

[12] Prasai, A.; Odendaal, W.G., "Utilizing stray capacitances of a litz wire," *Industry Applications Conference, 2005. Fourtieth IAS Annual Meeting. Conference Record of the 2005* , Vol. 3, 2-6 Oct. 2005, pp. 1876- 1883

[13] National Aeronautics and Space Administration. *Electrical Bonding for NASA Launch Vehicles, Spacecraft, Payloads, and Flight Equipment*, Washington, D.C., NASA, NASA-Std-4003.

[14] United States Department of Defense. *Requirements of the Control of Electromagnetic Interference Characteristics of Subsystems and Equipment.* Wright-Patterson Air Force Base, OH, United States Department of Defense, Mil-Std-461.

[15] United States Air Force, *Electromagnetic Compatibility Requirements for Space Systems,* Los Angeles, CA, USAF Space Division, Mil-Std-1541.

[16] United States Department of Defense. *Product Verification Requirements for Launch, Upper Stage and Space Vehicles*, El Segundo, CA, Space and Missile Systems Center, Mil-Std-1540.